Electronic Supplementary Material (ESI) for CrystEngComm.

Supplementary information

Constructing 2D/2D Heterojunction of $MoSe_2/ZnIn_2S_4$ Nanosheets for Enhanced Photocatalytic Hydrogen Evolution

Ting Feng, [a] Kaili Zhao, [a] Haiyan Li, [a] Wei Wang, [a,b] Bohua Dong,[*a] Lixin Cao [*a]

a School of Materials Science and Engineering, Ocean University of China, Qingdao, 266100, P. R. China

b Aramco Research Center-Boston, Aramco Services Company, Cambridge, MA 02139, USA

[*] Corresponding author.

E-mail address: caolixin@ouc.edu.cn (Lixin Cao), dongbohua@ouc.edu.cn (Bohua Dong).

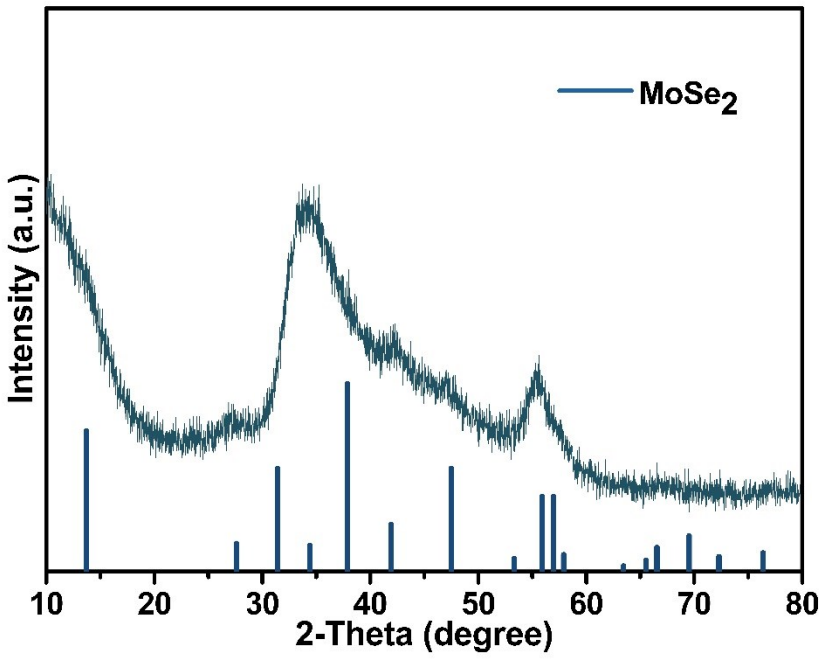

Figure S1. XRD pattern of $MoSe_2$

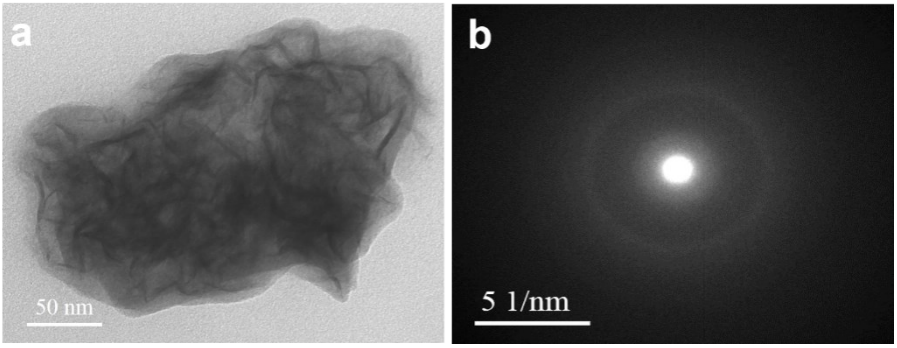

Figure S2. (a) TEM image and (b) the corresponding SAED pattern of $MoSe_2$

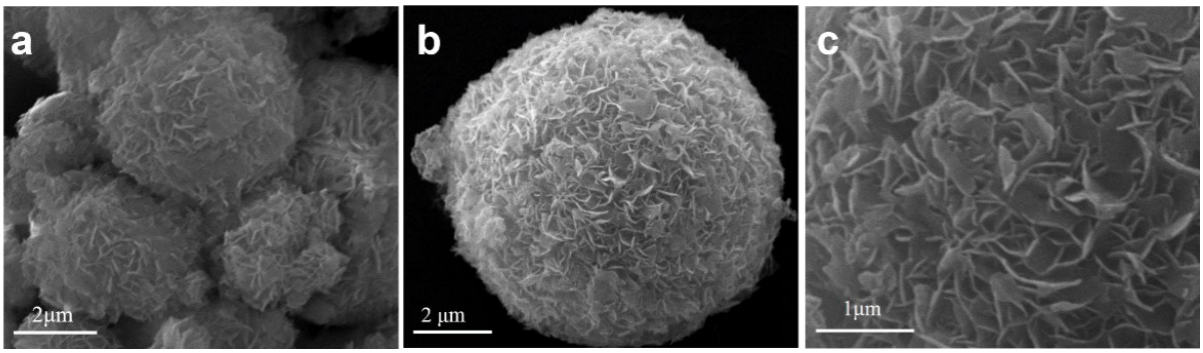

Figure S3. SEM images of $ZnIn_2S_4$ (a, b, c)

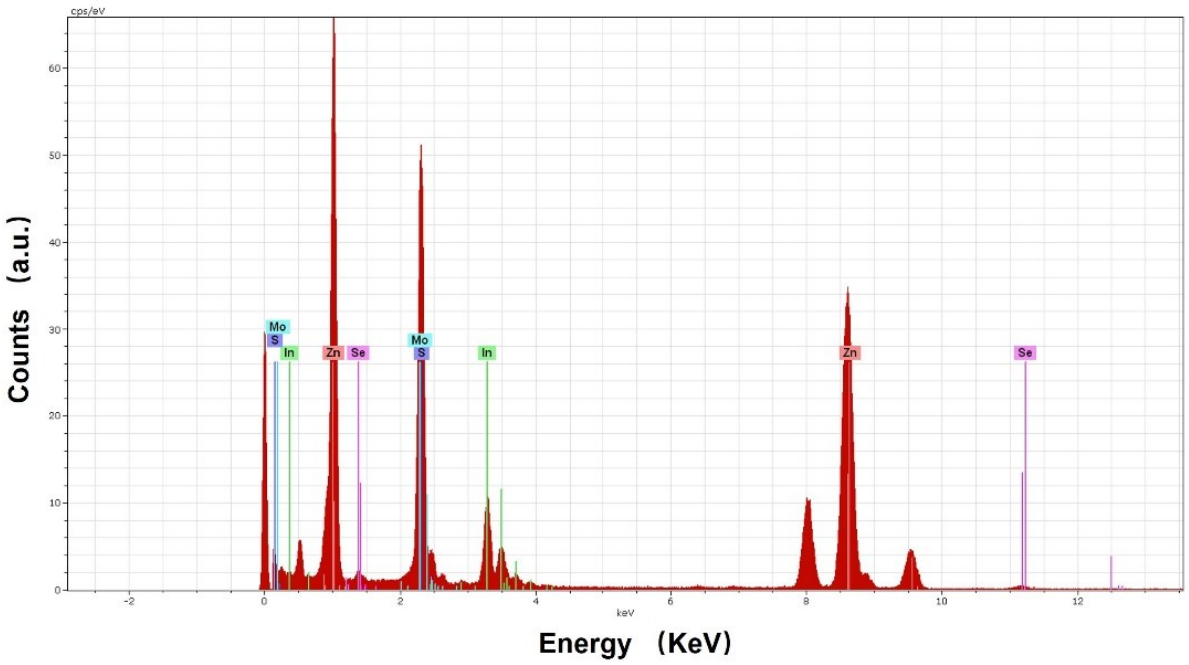

Figure S4. EDX spectrum of 10%$MoSe_2/ZnIn_2S_4$

Table S1. Metal elements ratio obtained by ICP and Brunauer-Emmett-Teller (BET) surface area data of these materials

Catalyst	Experimental Mass ratio (Mo: Zn)	BET surface area(m^2/g)
$ZnIn_2S_4$	-	93
10%$MoSe_2/ZnIn_2S_4$	1: 5.8	92
$MoSe_2$	-	44

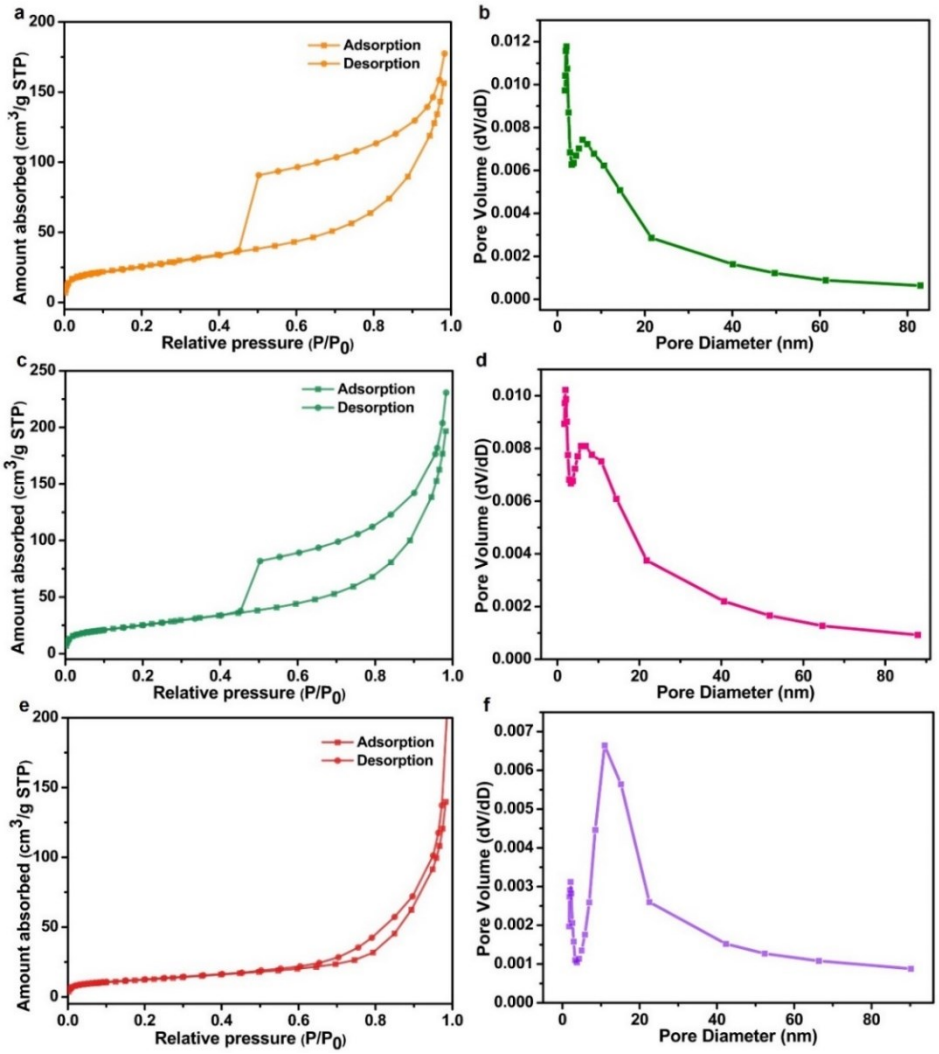

Figure S5. Nitrogen adsorption-desorption isotherms(left) and corresponding distribution plots about pore diameters (right): (a)(b) $ZnIn_2S_4$ nanosheets, (c)(d) 10%$MoSe_2$/$ZnIn_2S_4$ nanocomposites, (e)(f) $MoSe_2$ nanoplates.

All samples show typical characteristics of containing hole materials and have an obvious H3 hysteresis loop based on the isothermal adsorption of branched chain Barrett Joyner Halenda (BJH) method which can further analyze the pore size distribution (Figure. S5a, S5c, S5e). The aperture distribution range of $ZnIn_2S_4$ is observed to be 4-21 nm (Figure S5b), demonstrating that the size of the aperture is nonuniform and the average value is about 9.46 nm, while the aperture distribution range of 10%$MoSe_2$/$ZnIn_2S_4$ (Figure S5d.) composites is similar to that of pure $ZnIn_2S_4$. The average aperture value of it is around 12.60 nm. The pore size distribution of $MoSe_2$ is observed in the range of 4-22 nm (Figure S5f.) and the average is approximately 19.1 nm. The specific surface area of $ZnIn_2S_4$ and $MoSe_2$ are 93 and 44 $m^2\ g^{-1}$, respectively, while that of 10%$MoSe_2$/$ZnIn_2S_4$ is 92 $m^2\ g^{-1}$ (Table S1) which is almost the same as that of $ZnIn_2S_4$. The specific surface area of 10%$MoSe_2$/$ZnIn_2S_4$ is still high, implying that the 2D $MoSe_2$ nanosheets formed in the presence of $ZnIn_2S_4$ has larger surface.

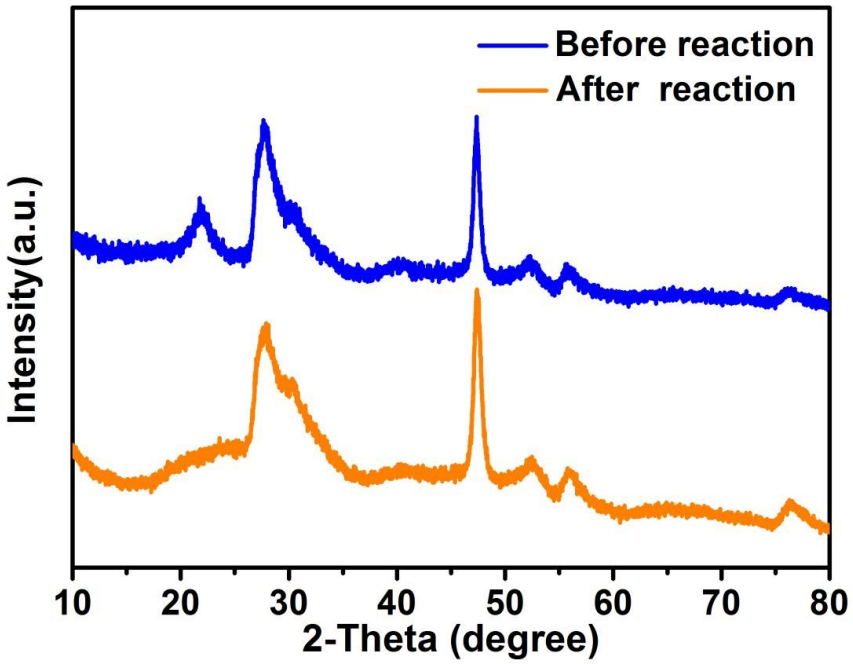

Figure S6. XRD patterns of 10% $MoSe_2/ZnIn_2S_4$ sample before and after photocatalytic reaction.

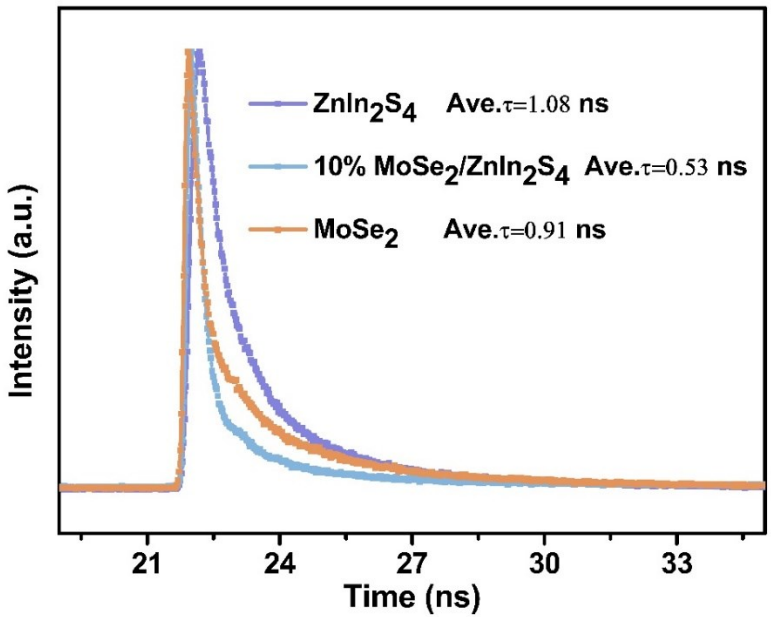

Figure S7 Transient-state photoluminescence spectra of $ZnIn_2S_4$, 10%$MoSe_2/ZnIn_2S_4$ and $MoSe_2$

Table S2 Fluorescence emission lifetime and relevant percentage Data of $ZnIn_2S_4$,10%$MoSe_2$/ $ZnIn_2S_4$ and $MoSe_2$

Samples	τ_1 (ns)	A_1 (%)	τ_2 (ns)	A_2 (%)	Average lifetime (τ_a) (ns)
$ZnIn_2S_4$	0. 74	60.32	3.52	39.68	1.08
10%$MoSe_2$/$ZnIn_2S_4$	0.40	74.0	7.53	26.0	0.53
$MoSe_2$	0.52	50.26	3.72	49.74	0.91

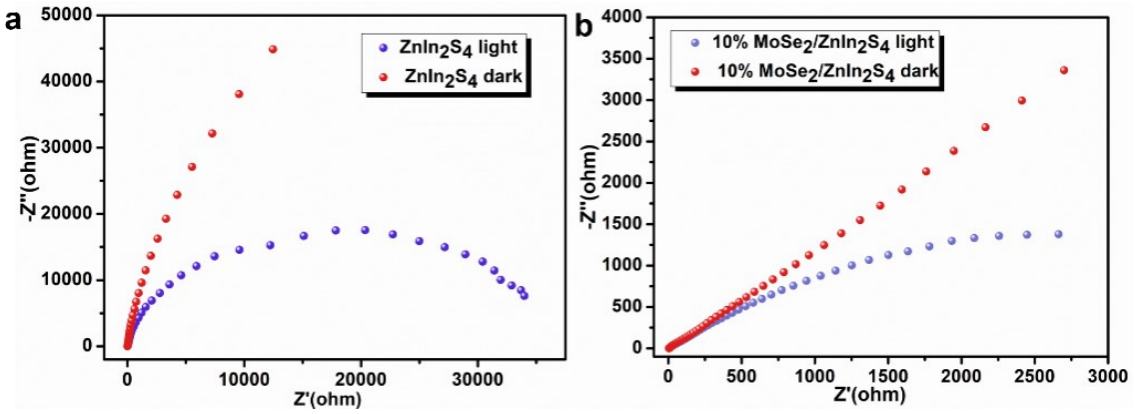

Figure S8. EIS Nyquist plots of $ZnIn_2S_4$ (a) and 10%$MoSe_2$/$ZnIn_2S_4$ (b)in dark and light condition.

The effects of switching on and off light on transfer resistance for different samples were compared in Figure S7. It can be seen that the arc radius of 10%$MoSe_2$/$ZnIn_2S_4$ samples decreases after irradiation, which indicates that light can effectively stimulate the transfer of internal electrons and holes. This further indicates that the electrons and holes of 10%$MoSe_2$/$ZnIn_2S_4$ can be transferred more quickly under switched light conditions.

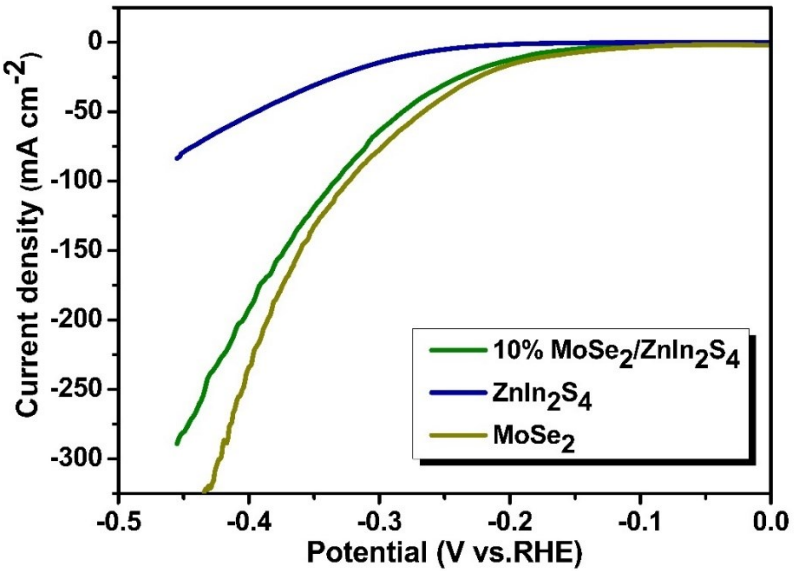

Figure S9. Linear sweep voltammetry (LSV) curves of $ZnIn_2S_4$, $MoSe_2$ and 10%$MoSe_2/ZnIn_2S_4$.

The linear sweep voltammetry curves of $ZnIn_2S_4$, $MoSe_2$ and 10% $MoSe_2/ZnIn_2S_4$ are compared in Figure S8, in which $MoSe_2$ and 10%$MoSe_2/ZnIn_2S_4$ composite exhibit higher cathodic current. At 10 mA cm^{-2} current density, the overpotential of $MoSe_2$ and 10% $MoSe_2/ZnIn_2S_4$ are 171 mV and 188 mV respectively, which are much lower than that of $ZnIn_2S_4$ (281 mV). LSV results show that the $MoSe_2$ can effectively reduce the overpotential of hydrogen production and 10%$MoSe_2/ZnIn_2S_4$ sample has a similar water reduction overpotential compared with $MoSe_2$, which indicates that $MoSe_2$ as a co-catalyst reduces the activation energy of the reaction and improves the performance of photocatalytic hydrogen evolution.

Table S3 Comparison of photocatalytic H_2 evolution rates of molybdenum-based cocatalyst modified $ZnIn_2S_4$ photocatalysts.

Photocatalysts	H_2 evolution rate (μmol h^{-1} g^{-1})	Scavenger	AQE/%	Light source (Xe lamp)	Reaction Temperature (℃)	Reference
$MoSe_2$/ $ZnIn_2S_4$	1226	0.35M Na_2S 0.25M Na_2SO_3	42.3(λ > 420 nm)	λ > 420 nm	6	**This work**
$ZnIn_2S_4$/MoS_2-RGO	425.1	20% lactic acid		λ > 420 nm	6	1
ZIS/MoS_2/CdS	7570.4	10 vol% TEOA	30.38(λ= 420 nm)	λ > 420 nm	25	2
$MoSe_2$/$ZnIn_2S_4$	2228	0.35M Na_2S 0.25M Na_2SO_3	21.39(λ= 400 nm)	λ > 420 nm		3
MoC-QDs/C/ $ZnIn_2S_4$	1131.9	10% lactic acid		λ > 400 nm	room temperature	4
Mo-doped $ZnIn_2S_4$	4620	10 vol% TEOA	14.74(λ= 420 nm)	λ > 420 nm	5	5
Au−MoS_2/ZIS	18955	0.35M Na_2S 0.25M Na_2SO_3		λ > 400 nm		6
Mo_2C/$ZnIn_2S_4$	7140	10 % TEOA	71.6 (λ= 420 nm)	λ > 420 nm	5	7
$MoSe_2$-$ZnIn_2S_4$	6545	10%lactic acid		λ >400 nm		8

The hydrogen evolution performance in our work is not excellent compared with other literatures. We speculate that there may exist some reasons resulting in the low photocatalytic activity. In this work, the system is a binary system **without noble-metal elements**. Noble metal or carbon could improve the conductivity of composite and accelerate electrons transfer. The crystallinity of co-catalyst and the separation of electrons are not getting the suitable balance. Poor crystallinity may make the material possess too much defects and the ability of trapping electrons becomes too strong which also results in less electrons taking part in the water reduction.

Reference

[1] Z.J. Guan, P. Wang, Q.Y. Li, G.Q. Li and J.J. Yang. Dalton Trans., 2018, 47, 6800.

[2] L. Wang, H.H. Zhou, H.Z. Zhang, Y.L. Song, H. Zhang, L.K. Luo, Y.F. Yang, S.Q. Bai, Y. Wang and S.X. Liu. Nanoscale, 2020, 12, 13791.

[3] D.Q. Zeng, L. Xiao, W.J. Ong, P.Y. Wu, H.F. Zheng, Y.Z. Chen and D.L. Peng. ChemSusChem 2017, 10, 4624-4631.

[4] F. Gao, Y. Zhao, L.L. Zhang, B. Wang, Y.Z. Wang, X.Y. Huang, K.Q. Wang, W.H. Feng and P. Liu. J. Mater. Chem. A, 2018, 6, 18979–18986

[5] F.S. Xing, Q.W. Liu, and C.J. Huang. Sol. RRL 2020, 4, 1900483

[6] G. Swain, S. Sultana, and K. Parida. Inorg. Chem. 2019, 58, 15, 9941–9955

[7] C. Du, B. Yan, G.W. Yang. Nano Energy 2020,76, 105031

[8] M. Q. Yang, Y. J. Xu, W. H. Lu, K. Y. Zeng, H. Zhu, Q. H. Xu and G. W. Ho. Nat. Commun., 2017, 8,14224.